Reversible Twinning in Pure Aluminum

B. Q. Li,[1] M. L. Sui,[1,*] B. Li,[2] E. Ma,[2] and S. X. Mao[3,†]

[1]*Shenyang National Laboratory for Materials Science, Institute of Metal Research, Chinese Academy of Sciences, Shenyang 110016, China*

[2]*Department of Materials Science and Engineering, The Johns Hopkins University, Baltimore, Maryland 21218, USA*

[3]*Department of Mechanical Engineering and Materials Science, University of Pittsburgh, Pittsburgh, Pennsylvania 15261, USA*

(Received 26 March 2009; published 20 May 2009)

Twinning in metals is normally a permanent plastic deformation mechanism. Here we report reversible twinning in high stacking fault energy (SFE) aluminum. Twinning and spontaneous detwinning at the crack tip have been captured *in situ* during tensile straining under a transmission electron microscope. Both the *in situ* observation and the molecular dynamics simulations reveal a two-stage detwinning process. The high propensity for detwinning is due to the high SFE and the low frictional forces against the detwinning partial dislocations in Al. This discovery of reversible twinning has implications for the deformation of other high SFE materials.

DOI: 10.1103/PhysRevLett.102.205504 PACS numbers: 62.20.D−, 62.20.F−

Twinning is an important mechanism for plastic deformation in metals. Among the face-centered-cubic (fcc) metals [1,2], pure Al is an intriguing case, as it rarely undergoes twinning due to its high stacking fault energy (SFE) [3–5]. Twinning in Al has thus attracted considerable attention in computer simulation studies [6–9] and in experimental investigations [8–11]. A recent claim of deformation twinning in Al [12] may have misinterpreted stacking faults and Frank loops [13] as microtwins, as explained in the supplemental materials [14]. Therefore, a careful monitoring of the detailed twinning process in Al remains important and challenging. In this Letter, using a combination of tensile straining and *in situ* high-resolution transmission electron microscopy (HRTEM), we have successfully captured the detailed dynamic twinning process in pure Al at the atomic scale.

Twinning is normally not reversible or recoverable, resulting in permanent strains. Interestingly, our *in situ* monitoring reveals a detwinning process that readily occurs, and in our Al case the twinning is entirely reversible. During the detwinning process, we found two stages: thinning of the twins and shortening of the twin boundaries (TBs). This observation is corroborated by our molecular dynamics (MD) simulations.

High-purity polycrystalline Al (99.999%) acquired from Goodfellow Inc. was used for the experiment. An electron backscatter diffraction (EBSD) micrograph of the as-received Al reveals a broad grain size distribution, ranging from several micrometers to 200 μm with an average grain size of ~65 μm [see Fig. 1(a)]. *In situ* TEM tensile specimens were thinned by double-jet electropolishing and then glued onto the center of a commercial Al substrate [15]. The room-temperature *in situ* tensile experiments were performed using a Gatan model 654 single-tilt straining holder, on a FEI Tecnai F30 TEM operating at 300 kV with a point-to-point resolution of 2.0 Å. Considering that the Al crystal is sensitive to electron irradiation, the electron beam was spread out during the intervals between taking HRTEM images, to minimize the beam damage. The tensile loading was controlled by applying pulsed displacement, and after each pulse the sample was held under stress for observation. After several initial incremental loading pulses, cracks nucleated and propagated in the thin area of

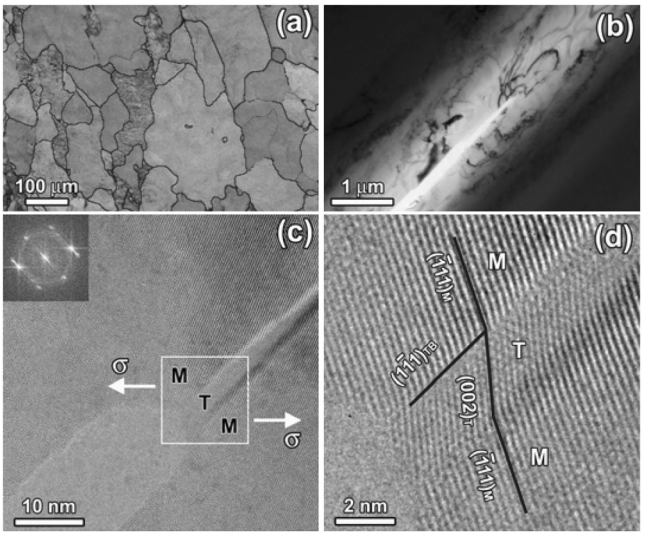

FIG. 1. (a) An EBSD micrograph showing the grain size distribution in the as-received polycrystalline pure Al. (b) TEM observation of the thin area produced by straining at the crack tip (marked by a white arrow). (c) Deformation twin (T) geometry and the loading direction relative to the crack plane. The inset shows the FFT pattern of the area ahead of the crack tip, indicating that the electron beam is close to the [110] zone axis. (d) HRTEM image of the twin (T) and the matrix (M) ahead of the crack tip. The twin boundaries are illustrated using solid lines, and the lattice planes of T and M are indexed.

the sample. Areas ahead of these cracks [see Fig. 1(b)] were chosen for TEM observation.

Figure 1(c) shows a HRTEM image of the deformed area ahead of a crack tip within a single grain, acquired after several loading pulses. At the crack tip, a deformation twin was observed with its TB plane parallel to the crack plane. The twin has a length of the order of 25 nm and a width of ~3 nm. From the fast Fourier transform (FFT) pattern [inset in Fig. 1(c)], the beam direction of the HRTEM image was close to a ⟨110⟩ zone axis (not exact because the titling was restricted in the single-title holder needed for the tensile loading). Based on both the loading condition and the viable slip system for the current twinning mode, the twinning dislocation is believed to involve a 90° partial ($\frac{1}{6}[\bar{1}12]$). The crystallographic planes involved are labeled in Fig. 1(d). During the holding period, although no more loading pulses were given to the sample, the sample was still in a loaded or strained state.

A series of HRTEM images, as shown in Fig. 2, were taken at the crack tip to monitor the twinning process. In Fig. 2(a), four ledges (steps) L_1–L_4 are found at the TBs. Under the tensile loading, all four ledges moved forward along the TBs, as shown in Fig. 2(b), and L_1 and L_3 advanced further in Fig. 2(c). Each of these ledges can be regarded as a bundle of twinning partial dislocations emitted from the crack tip, with the height of the ledge being equal to the number of accumulated partials [15,16]. The movement of each step thus involves the coordinated forward propagation of multiple partials on planes adjacent to the TBs [17]. This process leads to the lengthening and broadening of the twin. After a while, the upper TB becomes flat, and two ledges, labeled as L_5 and L_6 in Fig. 3(a), are developed on the lower TB.

We next present the interesting observation of detwinning. During further holding of the sample, stress relaxation occurred. The twin growth stopped as a result. Instead, we observe in Fig. 3 that the ledges turned around and marched back towards the crack tip. Comparing Figs. 3(a) and 3(b), the ledge L_5 moved all the way to the crack tip and disappeared to the surface (the twin thickness in that region thus shrinks from ~2.8 to ~1.6 nm), and another step L_7 came in from the right-hand side, approaching L_6.

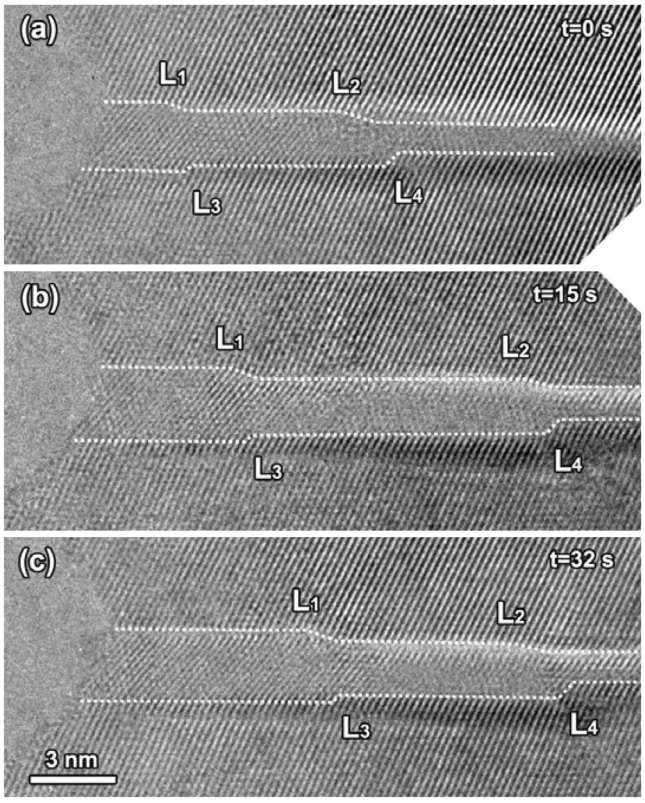

FIG. 2. A series of HRTEM images taken at different points of time (t), showing the twinning process at the Al crack tip. The TBs are outlined by dashed lines, and the progressing ledges on the TBs are indicated by L_1–L_4. (a) $t = 0$ s. (b) $t = 15$ s. (c) $t = 32$ s.

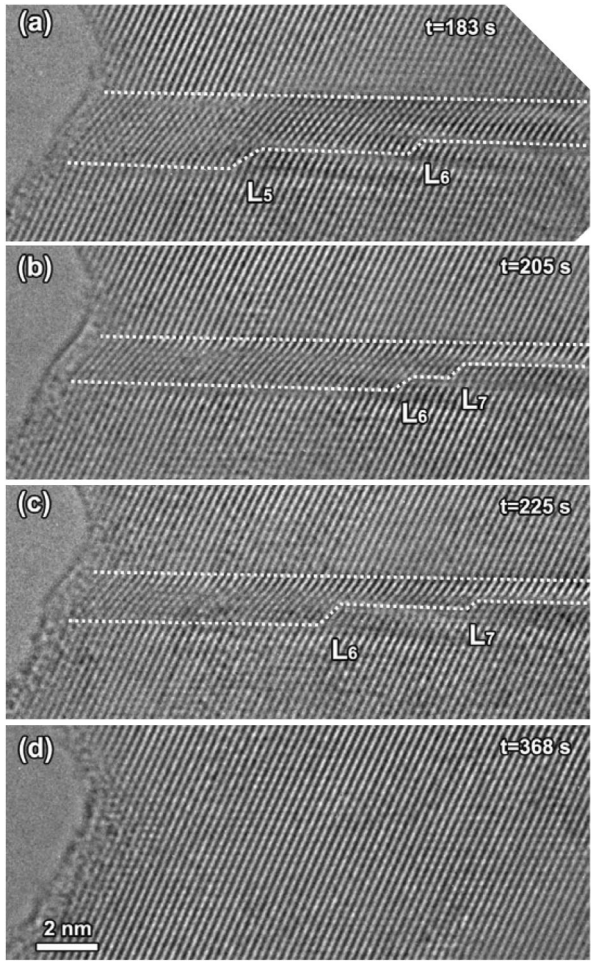

FIG. 3. A series of HRTEM images taken at different times, monitoring the detwinning process of the twin in Fig. 2. The TBs are outlined using dashed lines, and the retracting ledges on the TBs are indicated by L_5–L_8. (a) $t = 183$ s. (b) $t = 205$ s. (c) $t = 225$ s. (d) $t = 368$ s.

L_6 and L_7 kept moving with time, towards the crack tip; see Fig. 3(c). The already-thinned twin then quickly detwinned altogether. An image taken at 386 s into the experiment showed that the twinned region was completely transformed back to the matrix stacking [Fig. 3(d)], rendering the twinning anelastic. The entire detwinning process took less than 3 minutes.

The spontaneous and easy detwinning can be explained as follows. First, we point out that for Al, which has a high SF energy (SFE) [6,7,17], the twin formed tends to be small and extend not far from the crack tip. This is because the initial twin nucleus cannot travel very far into the sample [17], as the twinning partials drag behind them an energy-costly SF. To overcome this resistance requires the presence of high stresses, which decay fast with increasing distance from the crack tip [18]. As a result of the close proximity to the crack, the twin has a strong tendency to spontaneously detwin when the applied stress is relaxed or unloaded. The partials on the steps are pulled towards the surface by the image force, which is a function of distance (d) from the free surface [18]. Also, the small twin size makes it unlikely for the partials/twin to be locked by other defects such as grain boundaries (this happens, for example, in nanocrystals [10,11]) and dislocations. As the partials and steps move to the surface, the twin gradually becomes sufficiently thin that the remaining layers are able to detwin all at once, as shown in Fig. 3(c). This last stage of complete detwinning is driven by the elimination of the two TBs (TB energy $\sim$ one-half of the SFE) [17] and is therefore so rapid that it can be reproduced even on the time scale (nanoseconds) of MD simulations (details in Fig. 4 below).

Second, the Peierls barrier against the gliding of an existing detwinning partial dislocation on the TB plane is relatively low for Al: From *ab initio* modeling the athermal friction force against a partial is 120 MPa, a factor of 4 lower than that for a metal like Cu [17]. The image force acting on the partial would reach 120 MPa by itself, when $d = 5$ nm. In reality, detwinning by step/partial movement is thermally activated, rather than an athermal process, such that it is also expected to happen for $d > 5$ nm, with the aid of thermal fluctuation [19]. In comparison, for a metal like Cu with much lower SFE, the twins formed are much longer and thicker (we conducted similar crack tip *in situ* experiments for Cu; the TEM picture is not shown), and the frictional forces of the partials are large [17], such that the detwinning probability is much lower. This is consistent with the frequent observation of twins at crack tips in Cu (not shown).

MD simulations were carried out for pure Al, to corroborate the experimental observation of detwinning at 300 K near the free surface. The simulation employs embedded-atom method potentials for aluminum [20], and the simulation box has dimensions of $40 \times 20 \times 10$ nm, with a periodic boundary condition applied in the thickness dimension. In Fig. 4(a), which displays the [110] projection view, a six-layer twin ($\sim$10 nm long) is embedded inside the matrix, with one end at the free surface (only part of the simulation box is shown). In Fig. 4(b), we observe that detwinning occurs rapidly at 300 K, even on the MD time scale, in the absence of applied stress or strain. After 200 000 time steps (each step is 3.5 fs), the length of the twin is obviously reduced relative to its original length in Fig. 4(a). This observation is in agreement with that in Fig. 3(c), where it is shown that in the last stage of detwinning the thin twin disappears altogether rapidly and completely reverts back to the matrix stacking. The twin boundary energy appears to be the dominant driving force for this stage of the detwinning, since the SFE is very high in Al. In Fig. 4(c), a three-layer step was created on top of a six-layer twin (left arrow). With time going by at 300 K, the step gradually moves towards the free surface. As seen in Fig. 4(d) after 2.7 ns,

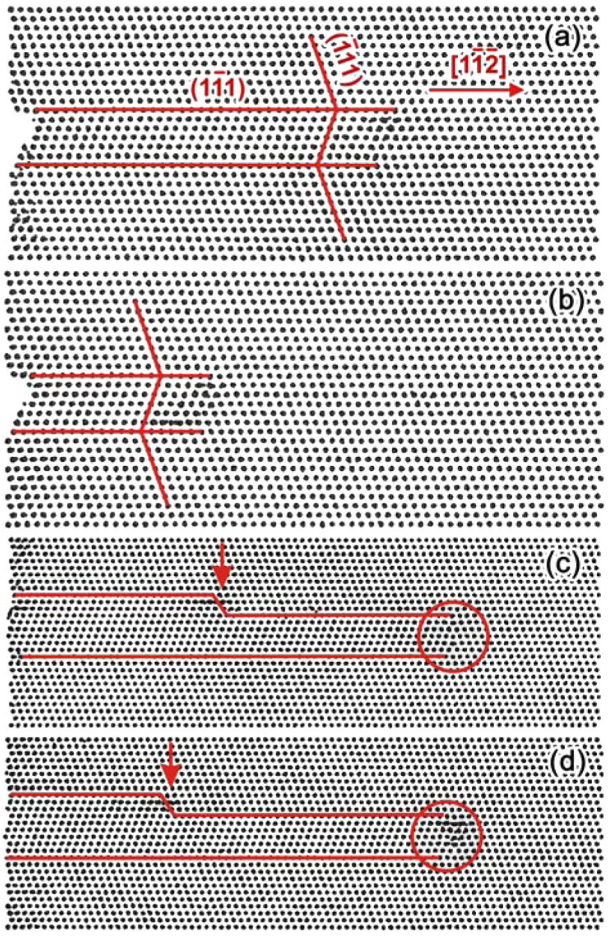

FIG. 4 (color online). (a) MD simulation model with [110] projection view; a six-layer twin ($\sim$10 nm long) is embedded inside the matrix, with one end at the free surface. (b) Detwinning at 300 K. (c) A three-layer step created on top of a six-layer twin (left arrow) gradually moves towards the free surface. (d) As the position of the three-layer step changes, the six-layer twin boundary starts moving (right circle).

an obvious change in position of the three-layer step can be identified. Meanwhile, as the three-layer step moves left, the six-layer twin starts moving (right circle). The observation in Figs. 4(c) and 4(d) is in agreement with that in Fig. 3(b), where it is shown that, in the first stage of detwinning, the twin is thinning or reducing its thickness via step movement at the TB. Here the movement of the partial dislocation(s) is driven mainly by the line tension of the partials (i.e., the image force). After the first stage of detwinning, the twin is now thinner, and all of the layers in the twin can now detwin together in the second stage. The latter can be completed more smoothly and quickly due to the newly joined driving force (twinning fault force) [19]. Here the image force is determined by the location of the partials, while the stacking/twin fault force is dominated by the SFE. For the high SFE materials such as Al, TB is a high energy planar defect with about half of the corresponding SFE, and the stacking fault force is large enough to overcome the Peach-Koehler force [19] and drive the twinning partials back to the crack tip to reduce the system energy. This insight suggests a high propensity for reversible deformation twinning in the high SFE materials. Therefore, we believe that reversible twinning could be a general and newly identified deformation mechanism for high SFE metals.

In summary, using *in situ* HRTEM tensile straining, convincing, atomic-scale evidence for reversible twinning (including both twinning and complete detwinning) at a crack tip in pure polycrystalline Al has been obtained. The reversible twinning process occurring in high SFE Al is different from conventional plastic deformation twinning normally found in low SFE metals. The reversible twinning process leaves no debris for postmortem observation. The detwinning is assisted by image force and thermal activation, and its apparent high propensity stems from the high SFE of Al and the low Peierls-Nabarro force against the motion of partials on the TBs.

B. Q. L. and M. L. S. acknowledge the support from the ''Hundred Talents Project'' of Chinese Academy of Science and the National Nature Science Foundation of China (Grants No. 10776032 and No. 50125103) as well as Chinese MoST Grant No. 2009CB623702. B. L. and E. M. are supported at JHU-CAMCS by ARMAC-RTP, DAAD19-01-2-0003, and W911NF-06-2-0006. S. X. M. acknowledges NSF CMMI-08-25842 through the University of Pittsburgh. We also thank Y. B. Wang and B. Wu for help in TEM operation and Professor W. Nix for valuable comments.

*mlsui@imr.ac.cn
†smao@engr.pitt.edu

[1] J. A. Venables, in *Deformation Twinning*, edited by R. E. Reed-Hill, J. P. Hirth, and H. C. Rogers (Gordon and Breach Science, New York, 1964), p. 77–116.
[2] J. W. Christian and S. Mahajan, Prog. Mater. Sci. **39**, 1 (1995).
[3] R. C. Pondand and L. M. F. Garcia-Garcia, Inst. Phys. Conf. Ser. **61**, 495 (1981).
[4] Q. Chen, Y. Huang, L. Qiao, and W. Chu, Sci. China E **42**, 1 (1999).
[5] D. H. Warner, W. A. Curtin, and S. Qu, Nature Mater. **6**, 876 (2007).
[6] D. Farkas, M. Duranduru, W. A. Curtin, and C. Ribbens, Philos. Mag. A **81**, 1241 (2001).
[7] S. Hai and E. B. Tadmor, Acta Mater. **51**, 117 (2003).
[8] V. Yamakov, D. Wolf, S. R. Phillpot, A. K. Mukherjee, and H. Gleiter, Nature Mater. **1**, 45 (2002).
[9] V. Yamakov, D. Wolf, S. R. Phillpot, and H. Gleiter, Acta Mater. **50**, 5005 (2002).
[10] M. W. Chen, E. Ma, K. J. Hemker, H. W. Sheng, Y. M. Wang, and X. M. Cheng, Science **300**, 1275 (2003).
[11] X. Z. Liao, F. Zhou, E. J. Lavernia, D. W. He, and Y. T. Zhu, Appl. Phys. Lett. **83**, 5062 (2003).
[12] W. Z. Han, G. M. Cheng, S. X. Li, S. D. Wu, and Z. F. Zhang, Phys. Rev. Lett. **101**, 115505 (2008).
[13] X. L. Wu, B. Li, and E. Ma, Appl. Phys. Lett. **91**, 141908 (2007).
[14] See EPAPS Document No. E-PRLTAO-102-017923 for supplemental discussions on the previous claims of TEM observation of twinning in pure aluminum. For more information on EPAPS, see http://www.aip.org/pubservs/epaps.html.
[15] Y. B. Wang, M. L. Sui, and E. Ma, Philos. Mag. Lett. **87**, 935 (2007).
[16] J. P. Hirth and R. W. Balluffi, Acta Metall. **21**, 929 (1973).
[17] S. Ogata, J. Li, and S. Yip, Phys. Rev. B **71**, 224102 (2005).
[18] E. B. Tadmor and S. Hai, J. Mech. Phys. Solids **51**, 765 (2003).
[19] J. R. Rice and G. E. Beltz, J. Mech. Phys. Solids **42**, 333 (1994).
[20] A. F. Voter and S. P. Chen, Mater. Res. Soc. Symp. Proc. **82**, 175 (1987).